JTTEE5 17:263–274
DOI: 10.1007/s11666-008-9177-1
1059-9630/$19.00 © ASM International

An Integrated Investigation Approach for Coating Temperature Measurement and Control During Plasma Spraying

Haiou Zhang, Weisheng Xia, Guilan Wang, Yunzhen Yang, and Yang Zou

(Submitted June 29, 2006; in revised form August 27, 2007)

An integrated investigation approach for temperature measurement and control of plasma sprayed coating is presented in this paper. It is based on infrared (IR) pyrometry combined with specific robot scanning trajectories. The temperature evolution was continuously detected and recorded during preheating, spraying, and cooling stages. Then the two specific factors, periodic average temperature and periodic standard deviation, were adopted to evaluate the temperature variation and the fluctuation of the thermal cycle relevant to one spraying period. These two factors were successful in describing the temperature variation during experimental processing sets. Moreover, the influence of processing parameters of Z-type robot spray trajectory, including spray distance, scanning velocity, and scanning step on coating temperature is experimentally researched and explained reasonably by comparing the two factors.

Keywords atmospheric plasma spray, diagnostics, IR pyrometry, process control, process monitoring, robot trajectory, spraying parameters, substrate/coating temperature

1. Introduction

The temperature and velocity of sprayed particles prior to their impact onto the substrate surface and the temperature history of substrate/coating are important parameters influencing the formability and quality of thermally sprayed coatings (Ref 1-4). However, the relationship between the temperature history and the properties of thermal sprayed coatings is still unclear. It has been emphasized that the monitoring of particle parameters at impact and coating temperature is a key issue for coating quality, reliability, and reproducibility (Ref 5, 6). Therefore, many efforts have been devoted to research on the monitoring and control of coating temperature.

To the knowledge of the authors, coating temperature can be measured during spraying by using various means: thermocouples (Ref 7-9), infrared (IR) pyrometry (Ref 10-15), pulse thermography (Ref 16), infrared thermal cameras (Ref 11, 13, 17), and other specially designed infrared thermal nondestructive testing (NDT) scanning systems (Ref 18). Although thermocouple measurement is a regularly applied and simple method that works well in a wide temperature range, the lack of good thermal contact to the surface being measured still remains an unresolved problem and leads to formation of the temperature gradients between thermocouple and sample. During the on-line temperature monitoring of plasma sprayed parts, thermocouples must be embedded in the substrate below the sprayed coating or placed at the edge of the substrate surface. It would be difficult or impractical to install them without covering the substrate or interfering with the surface pattern. Hence, thermocouple measurement is always applied in the calibration of noncontact temperature measurement methods.

As a whole, IR pyrometry has a wider application in industry (Ref 19-22) as a noncontact and nondestructive examination method. With the help of IR thermal cameras it was easy to visualize the temperature field of large area parts (Ref 11, 17, 23). However, it can be difficult to use these cameras in the presence of the intense plasma luminous radiation. Furthermore, more time is required to perform the thermographic data analysis by a skilled operator or by an automatic device to obtain the pertinent information (i.e., coating damage, defects) for process control. These factors reduce the real-time and on-line performance of the monitoring system using thermal cameras. However, IR thermal camera has proven to be an acceptable approach for monitoring temperature while spraying small and thin products made of aluminum, plastics, and composites used in the aerospace industry (Ref 17, 19). It is also helpful for the process diagnosis of the temperature field in special operating conditions (Ref 24). As a single spot device, IR pyrometer requires less time to analyze measurement data. Moreover, it can

Haiou Zhang and **Weisheng Xia**, State Key Laboratory of Digital Manufacturing Equipment and Technology, Huazhong University of Science & Technology, Wuhan 430074, China; and **Weisheng Xia, Guilan Wang, Yunzhen Yang,** and **Yang Zou**, State Key Laboratory of Material Processing and Die & Mould Technology, Huazhong University of Science & Technology, Wuhan 430074, China. Contact e-mail: xiatianhust@hotmail.com

be used in the on-line monitoring of coating temperature without keeping the plasma jet away or even suspending the spraying process during plasma spraying if one takes account of the relevant influencing factors. These factors are the substrate and coating emissivities, the wavelength range, and the absorption effects of the surrounding air, the plasma emission, and others. However, this is not the case for the thermal camera. Therefore, it is more reasonable and necessary to study the process control and diagnosis of sprayed coating temperature based on the combination of IR pyrometer and thermal camera, which is also the research focus in our laboratory.

Many research efforts have been performed on dealing with the temperature monitoring and control of plasma sprayed coatings by IR pyrometry. The published literature discusses details for monitoring of substrate and coating temperatures by IR pyrometry and the factors influencing the measurement (Ref 14, 25). Lugscheider et al. have monitored the temperature evolution of a button-type sample with a Keller pyrometer and a thermocouple and accordingly adjusted the cooling capacity to achieve a constant substrate temperature of 375 °C (Ref 21). Jokinen et al. determined the correlation between the mechanical properties of coating and the temperature history during high-velocity oxyfuel (HVOF) process with the help of the in situ temperature control based on the thermal camera (Ref 11). The spray and deposit control (SDC) system has been applied to detect the substrate/coating temperature time evolutions by IR pyrometry and simultaneously the beam deflection caused by stresses generated within the coating and substrate during spraying. This SDC has proved to be a successful technique to monitor the thermal spray process (Ref 26, 27). The French Atomic Energy Agency (CEA) has developed a diagnostic apparatus to measure the heat flux in temperature-controlled plasma spray process (Ref 28). The coating temperature was adjusted by controlling positive and negative (cooling) heat fluxes. Implementing this device, Meillot et al. have successfully deposited oxygen-sensitive materials on heat-sensitive substrates (Ref 29). Bao et al. have done simulations and experimental investigations on the influence of operating parameters on the heating of substrate and coating through temperature fluctuations at two fixed points of the substrate: one at the center and the other at the edge (Ref 30).

Therefore, to develop a new measurement approach using IR pyrometry, much attention should be paid to the previous systematic research ranging from monitoring coating temperature and processing and analyzing measurement data to controlling coating temperature distribution and also investigating the influence of the temperature history on mechanical and in-service properties for a specific coating.

In this paper, the substrate/coating temperatures were measured by an IR pyrometer moved with the robot holding the spray torch. Accordingly, the temperature history of substrate/coating can be recorded by this pyrometer during preheating, spraying, and cooling stages. Within one robot spraying cycle, an average value and a standard deviation are calculated from the in situ temperature values. These two factors were selected to evaluate the temperature fluctuations from one spraying condition to another or to evaluate the temperature evolution during time (more than one spraying cycle). A series of experiments were carried out to prove that these two factors give a good indication of the coating temperature fluctuations during plasma spraying. Finally, the influence of robot spray trajectory parameters on coating temperature, including spray distance (H), scanning velocity (V), and scanning step (D), was systemically investigated by comparing the differences of the two factors under different selected spraying conditions.

2. Experimental

2.1 Temperature Measurement Device and Method

The pyrometer used in this study is a monochromatic IR pyrometer Thermalert TX (Raytek Inc., Santa Cruz, CA, USA) with a response time of 165 ms. It operates in the 8 to 14 μm wavelength range where the absorption effect of the surrounding atmosphere as well as the reflected plasma emission are negligible (Ref 23, 31). The pyrometer allows temperature measurement from –18 to 300 °C, and the tolerance of ±1% of the measured temperature is specified by the pyrometer manufacturer (Ref 32). Its focusing distance is 1524 mm, the focused spot size is 46 mm, and the spot size at sensor is 18 mm.

The IR pyrometer only provides local temperature information and cannot measure the temperature gradient on a large area without a special scanning mechanism moving the point of the measurement on the part to be measured (Ref 11). Another possibility is to use a line scanner, an IR thermal camera, or arrays of single spot pyrometers all aiming at different locations along the surface of sprayed samples. Therefore, the pyrometer was fixed on the end arm of six-axis robot (MOTOMAN UP20, Shougang Motoman Robot Co., Ltd., Beijing, China) and synchronously moved with the plasma gun. This case can provide the pyrometer the special scanning mechanism to enlarge its detecting scope and flexibility. The geometrical dimension of the pyrometer is 187 × Φ42 mm with the optical resolution of 33:1 and the weight of 330 g, so the measurement does not influence the movement of the spray robot and also cannot be disturbed by the passage of plasma gun.

A schematic diagram of temperature-monitoring system during plasma spraying is presented in Fig. 1. For temperature measurements during spraying, the pyrometer spot was aimed at a point, with a presetting distance (usually equal to the scanning step) away from the centerline of the plasma gun. There is a viewing angle (β in Fig. 1) between the centerline of the pyrometer and the perpendicular of the substrate. This angle can be adjusted to keep the plasma jet off the optical passage of the pyrometer, if the spray jet axis position changes at the different operating conditions. The pyrometer can be adjusted along its centerline to keep its measurement distance (210 mm in this study) constant with the spot size of 22 mm as the spray distance is varied. The experimental setup in plasma spraying is shown in Fig. 2. In this study,

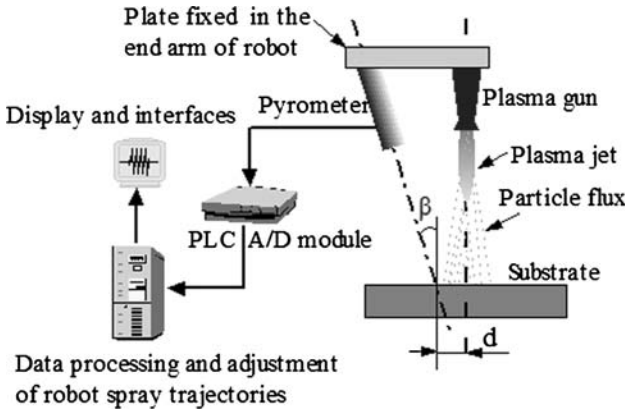

Fig. 1 Temperature-monitoring system during plasma spraying

Fig. 2 Experimental setup with the pyrometer and plasma torch on the same robot arm

the distance between the centerline of the torch axis and the spot of the pyrometer is fixed at 10 mm, and the viewing angle is 15°.

A schematic diagram of the Z-type robot spray trajectory is shown in Fig. 3, which represents the path of the center of the plasma jet. In this figure, L_x and L_y stand for the dimension of the entire spraying scope, and D is the scanning step (distance between two adjacent passes over the sample parts). If the path of the plasma gun from the end point to the start after a full scanning is in the scope of the sprayed parts, damage would occur due to the repeated heat input and coating buildup. Hence, the departure distance d_x is arranged. In this paper, the spraying cycle is defined as one full movement of the plasma gun from the start point to the end, and then to the start, as shown in Fig. 3. The elapsed time of one spraying cycle is regarded as a spraying period.

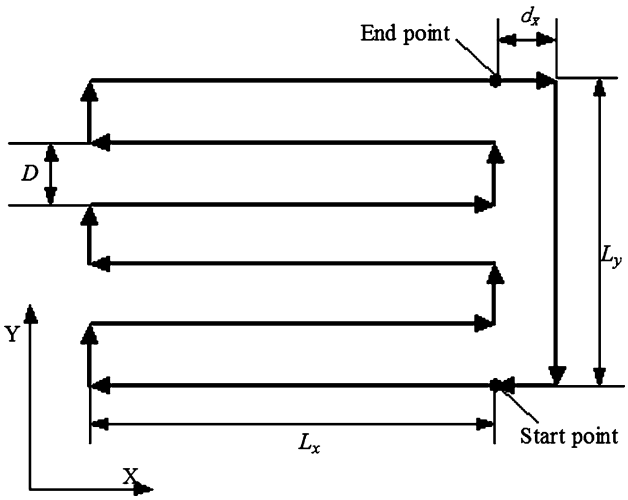

Fig. 3 Z-type robot spray trajectory

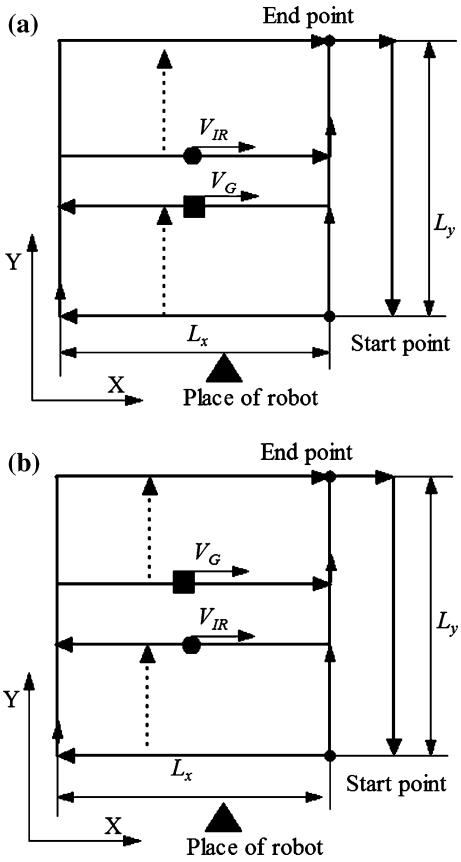

Fig. 4 Two configurations for coating temperature measurement

As for the different relative positions between plasma gun and IR pyrometer, there are two measurement configurations; these are referred to as before plasma gun (Fig. 4a) and after plasma gun (Fig. 4b), respectively. For the configuration before plasma gun, the value detected by the pyrometer corresponds to the substrate temperature

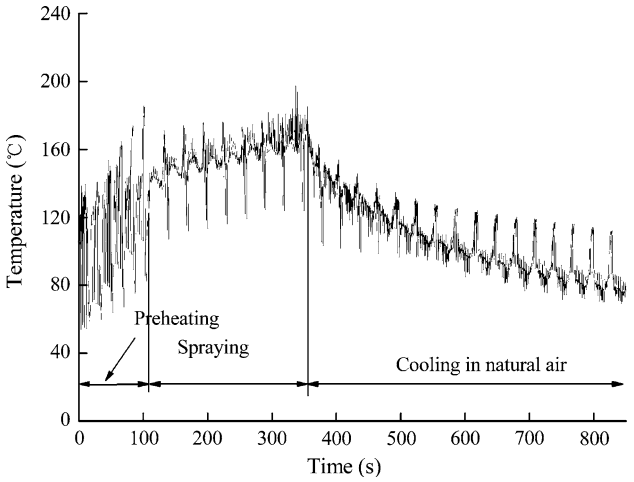

Fig. 5 Typical temperature evolution from in situ measurement data during preheating, spraying and cooling stages of APS process

during the preheat cycles when no coating is being deposited and to the surface where coating will be deposited in subsequent coating passes. In the second configuration, the pyrometer measures the coating temperature after spraying.

In this study, the configuration before plasma gun is applied. Robot moves cyclically from the start to the end along the trajectory illustrated in Fig. 3, and the substrate and coating temperatures are continuously monitored and recorded by the pyrometer. Thus, a reproducible cycle is achieved after each robot spraying cycle. Finally, constant repeatable temperature cycles during different stages can be obtained. A typical temperature curve from the in situ measurement data during the APS process including preheating, spraying, and cooling stages is shown in Fig. 5. The time 0 s means the start of the preheating stage. There are repeatable temperature cycles for the different stages, and each cycle represents a spraying cycle throughout the target sample. Counting the number of cycles allows determination of the number of full scans and deduction of the time for spraying. Preheating of the substrates by plasma jet was performed for six cycles prior to deposition. It can be observed from the peaks and troughs in Fig. 5 that there are large fluctuations for the preheating stage, while there are smaller fluctuations for the spraying stage and smallest for the cooling stage.

The temperature fluctuation information of the previous several spraying cycles is used to establish the corresponding feedback control strategies, such as cooling with compressed air, holding the spraying process temporarily, or switching the spraying trajectory, are determined and applied for the upcoming cycle.

2.2 Compensation for Emissivity Change at Various Conditions

Generally, the temperature measurement by IR pyrometer is influenced by the emissivity of the targets (varying with substrate roughness, temperature, and material, etc.), plasma emission, thermal radiation of sprayed particles, absorption of dust, and other factors (Ref 4). In the past, Madura and Piatkowski (Ref 33) presented a new emissivity compensation algorithm of temperature measurement devoted to metal objects with minimum error for double-bank pyrometry. Computer simulations of the method are carried out for Al, Fe, Cr, Cu, and also for two kinds of bricks. Moulla et al. has presented a method to study the influence of reflected atmospheric plasma spray (APS) torch radiations on long wavelength (7.5-13 μm) IR radiometry temperature measurement (Ref 34). They find that reflected APS torch radiation has a dramatic influence in case of low target temperature or low target emissivity. Chen et al. (Ref 35) have proposed a design principle for simultaneous emissivity and temperature measurements.

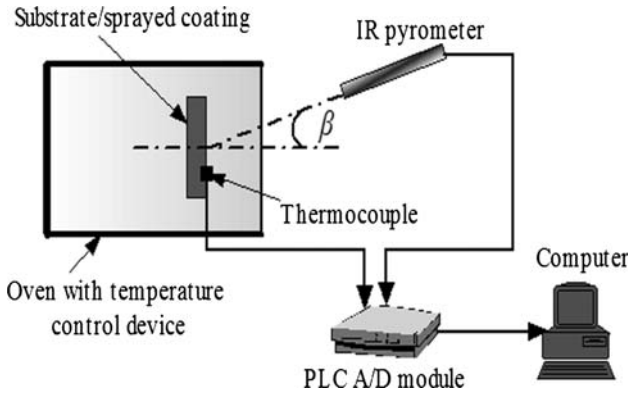

Fig. 6 Experimental setup for emissivity measurement

As for the APS process in our laboratory, the emissivity of coatings is not always the same as that of substrates, and it also varies with different temperature and thickness during plasma spraying. Hence, the variation of emissivity must be taken into consideration to correct the final measurement results during the processing of temperature data. The choice of the sample emissivity was determined according to the user manual accompanying the device. If there was no reliable reference for the specific substrate or coating material, its emissivity value was determined by the calibration method. The emissivity measurement apparatus is schematically illustrated in Fig. 6. The temperature in the oven was controlled by a control device from room temperature to 600 °C. Output from the pyrometer and the K-type thermocouple (DM-6801A, Victor Hi-Tech. Co., Ltd., Shenzhen, China) were sampled by the PLC A/D module (S7-300, Siemens Ltd., China) and then processed by the computer. Although the emissivity of most materials is not strongly dependent on viewing angle provided the measurement is made within about 45° of normal, the same angle β (Fig. 1) is still designed between the axis of the pyrometer and the vertical line of the substrate or sprayed coating in Fig. 6. During the calibration process, a sample of the material is heated to a known temperature determined by the contact thermocouple. Then the target temperature was measured with the IR pyrometer. The emissivity of the pyrometer is

adjusted until its temperature corresponds to that of the thermocouple. Finally, the emissivity is recorded for all future measurements of targets on this material at this temperature.

According to the Stefan-Boltzmann radiation law (Ref 36), the total radiation intensity of real body surfaces is:

$$M(T,\varepsilon) = \varepsilon \cdot \sigma \cdot T^4 \quad \text{(Eq 1)}$$

where σ is Stefan-Boltzmann constant, T is thermodynamic temperature, and ε is the emissivity of the object.

The temperature difference ΔT is defined $\Delta T = |T_1 - T_0|$, and the emissivity difference $\Delta\varepsilon$ is $\Delta\varepsilon = |\varepsilon_1 - \varepsilon_0|$, so the temperature value is corrected:

$$\frac{\Delta T}{T_0} = 1 - \left(1 - \frac{\Delta\varepsilon}{\varepsilon_1}\right)^{1/4} \quad \text{(Eq 2)}$$

where T_0 is the initial measuring temperature corresponding to the emissivity value ε_0, and T_1 is the temperature after the emissivity correction value ε_1.

In this study, the emissivity calibration test was carried out over the temperature range from room temperature to 300 °C. The mean value calculated from the test results is used in the compensation method above to correct the measured temperatures. It is worth noting that the effects of molten particles in plasma jet and plasma radiation were not taken into account during the measurement.

2.3 Analysis of the Present Temperature Measurement Methods

Besides the factors mentioned previously, other important factors influencing the measurement precision and the implementation field of the method presented in this paper are robot scanning velocity, the response time of the pyrometer, and the dimension of target parts. Unlike thermal imaging, IR pyrometer cannot give the temperature distribution immediately, so the temperature distribution is mapped after a full scan of the entire spraying scope. Hence, it will take longer to perform a scan with lower scanning velocity of robot for the sprayed part with a fixed dimension. In this case, it cannot reach the approximate real-time temperature distribution of the target coating by this measurement method due to the heat dissipation; however, the heat loss by radiation and convection can be reduced by altering the atmosphere surrounding the spraying coating. Moreover, to map the temperature distribution, many possible measurement data are beneficial. So the pyrometer with fast response time is better and allows a fast scan of a target in a few seconds. Therefore, the application of this temperature measurement method needs to take optimal robot scanning velocity and the reasonable response time of the pyrometer into consideration to obtain the approximate real-time temperature distribution. It is the best choice for a part with a small area, which can be fully scanned in about 20 s by the pyrometer with a response time of 165 ms and the robot scanning velocity of 400 mm/s. A larger spray area, approaching that of industrial parts, could be accommodated by using a robot with faster scanning velocity and a pyrometer with faster response time.

2.4 Processing of in situ Temperature Data

Since there are so many data points, peaks, valleys, and different fluctuations in the temperature curve from the in situ measurement during a long spraying time, it is difficult to distinguish the characteristic information for on-line process control. Furthermore, more time would be spent on the data processing for a computer, and also it is impossible to realize the real-time control of coating temperature distributions based on the measurement approach.

To investigate the real-time fluctuation of coating temperature, the periodic average temperature was chosen to indicate the temperature increasing or decreasing trends of the entire spraying scope, and the periodic standard deviation was selected to scale the temperature fluctuation during a scanning cycle on the basis of the statistical methods. The average temperature TA_i and the standard deviation TSD_i were determined as follows, respectively:

$$TA_i = \sum_j T_{ij}/n \quad 1 \le j \le n \quad \text{(Eq 3)}$$

$$TSD_i = \sqrt{\sum_j (T_{ij} - TA_i)^2/n} \quad 1 \le j \le n \quad \text{(Eq 4)}$$

where, T_{ij}, i, and j stand for time-varied temperature value, the number of scanning period, and the number of the temperature value of the period, respectively, and n is the total number of sampling data within one scanning cycle.

When the periodic standard deviation has an abnormal fluctuation compared with those of previous scanning cycles, the temperature isotherm will be created to analyze the temperature distribution based on in situ temperature values and corresponding robot positions. Coating temperature isotherm of one spraying cycle during plasma spraying is shown in Fig. 7. According to the contour, the

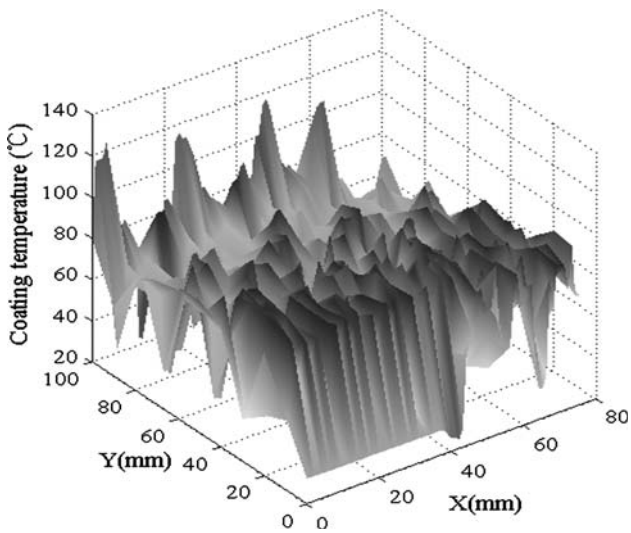

Fig. 7 Coating temperature isotherm of one spraying cycle during plasma spraying

local high- and low-temperature areas of the coating surface are distinguished, and also the coordinates of the specific area among the spraying scope are determined and provided to the monitoring system. After this, the feedback control strategies, such as cooling by natural convection, holding of spraying process, heating of local lower temperature area by the plasma jet without powder feeding, and so forth—in other words, strategies to adjust the temperature—are carried out to eliminate the nonuniformity of the temperature distribution by the algorithm. Meanwhile, the maximum value and the minimum one have to be taken into consideration for the closed-loop control of coating temperature, especially for the spraying of oxygen-sensitive or low melting point material on the heat-sensitive substrate.

2.5 APS Process

The commercially available Ni-base powder used in this study was ZX.Ni45 (0.5C-3.8Si-2.5B-12Cr-4Fe-bal Ni) (wt%) provided by the manufacturer (Zhenxing Inc., Chengdu, China), in the 56 to 20 μm particle size range. Mild steel plates (Q235) of size 100 × 110 × 4 mm were selected as substrates. They were previously grit blasted and cleaned in acetone prior to spraying. The grit-blasting material was corundum with the particle size of 83 to 840 μm, and the other conditions included gas pressure (6.5 MPa), distance (120 mm), and angle (90°). Other ceramic substrates of size 120 × 80 × 15 mm were also used, which consisted mainly of a composite powder mixed with ceramic and metal powders (Ref 24). Experimental trials were carried out with a Metco 9MB gun under ambient atmosphere. All experiments are based on the operating parameters listed in Table 1, unless otherwise specified. The calibrated coating emissivity deposited with the Ni-base powder above is 0.82 (standard deviation is 0.04).

To investigate the influences of robot spray trajectory parameters, such as spray distance, scanning velocity, and scanning step on coating temperature in APS, experimental sets were carried out keeping substrates and environment to room temperature before spraying, provided the effect of the spray environment on the experimental results was constant. The temperature was continuously monitored and processed for about 3 to 4 min according to the method described previously. Due to the different corresponding spraying periods for different spray velocities and scanning steps, the x-axis of the figures describing experimental results, spraying time is rearranged according to the number of spraying cycles and their relative periods, so that the variations of average temperature and fluctuation can exhibit the different influence for different spray trajectory parameters at the same time.

Table 1 Atmospheric plasma spray parameters

Parameter, unit	NS(a)	DS(b)	PE(c)
Arc current intensity, A	450	480	400
Powder feeding rate, g/min	11.04	20.58	4.56
Spray distance, mm	150	130	100 150 **200** 250
Scanning velocity, mm/s	300	200	50 **100** 150
Scanning step, mm	10	16	5 **10** 15

Nozzle exit internal diameter, 8 mm; feedstock injector diameter, 1.8 mm; voltage, 50 V; Prime plasma gas flow rate (Ar), 25 sLpm; Powder carrier gas (N_2), 3.5 sLpm. (a) NS for the normal spraying process. (b) DS for the spraying process with the damage phenomenon. (c) PE for the experiment sets investigating the influence of robot spray trajectory parameters on coating temperature distribution, and values in bold belong to the reference condition

3. Efficiency Validation of the Two Specific Factors

The group NS of spraying parameters listed in Table 1 was used for the experimental validation of the normal spraying process and DS for the spraying process with coating damage. To validate the efficiency of the two specific factors, many experimental sets were carried out with different substrates under different operating conditions, which included normal spraying processes and others with damage phenomena occurring in the manufacturing process. Because the typical common results listed as follows have been obtained in previously designed experimental sets, there is only one example for each process illuminated in this paper.

3.1 Normal Spraying Process

A ceramic substrate was preheated at 300 °C in a furnace before spraying. The spraying period was 19 s, and substrate and coating temperatures were continuously monitored by the pyrometer. As shown in Fig. 8, the period of the temperature curve is 19 s, which is the same as the robot spraying period, and thus the length of the spray time can be deduced according to the number of temperature cycles. The temperature curve has a high upward slope at the beginning of spraying due to the accumulation of heat input from plasma jet and spray particles during the spraying process. However, the slope then begins to slow down after 120 s because the thermal

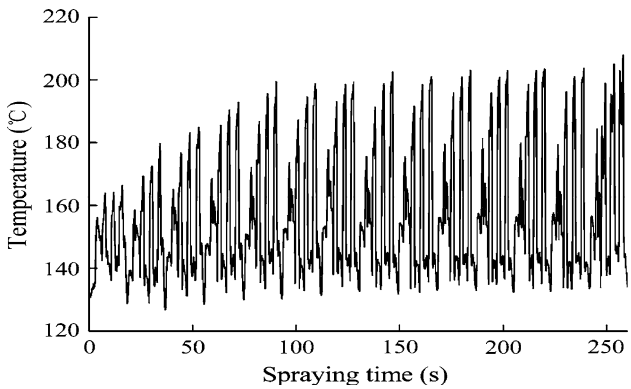

Fig. 8 Temperature curve versus time during plasma spraying process

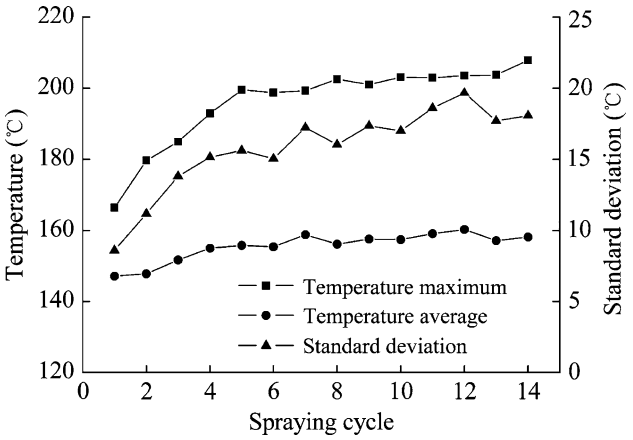

Fig. 9 Variations of the specific factors during the normal spraying process

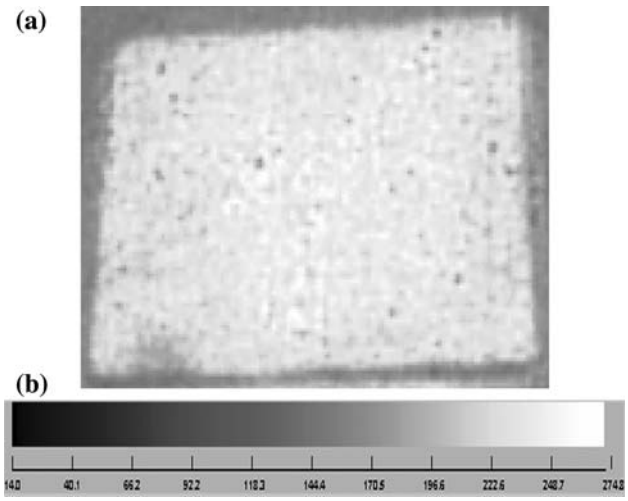

Fig. 10 Temperature field of the substrate before spraying (a) and its thermometric scale (b)

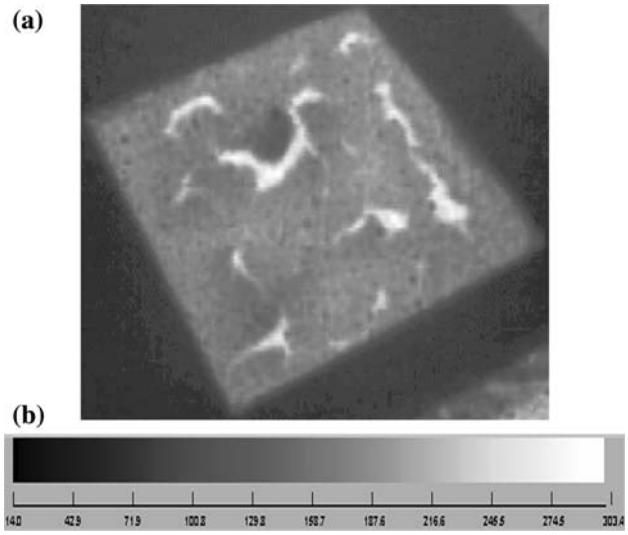

Fig. 11 Temperature field of the sprayed coating with damage during spraying (a) and its thermometric scale (b)

transfer coefficient and the thermal exchange ability of the sprayed metal coating are higher than that of the ceramic substrate, and consequently the heat is reduced. When the spray time is more than 180 s, the temperature fluctuation is almost constant. This is caused by almost dynamically steady heat exchange between the plasma power, the sample, and the circumstance.

The same conclusions above can be easily obtained from Fig. 9, which is composed of periodic average temperatures, maximum values, and standard deviations. As shown in Fig. 9, the periodic average temperature has a small fluctuation during the first five spraying cycles, but the standard deviation has a larger fluctuation as well as the temperature maximum. After that, there are no large differences for all the factors. During the spraying process, no damage occurred due to the almost steady average temperature and the slight fluctuation of standard deviations.

3.2 Spraying Process with Damage Phenomenon

Before spraying, the mild steel substrate was preheated at 300 °C in a furnace. To deeply investigate coating damage phenomena, the thermal camera HY-2188G (Huazhong Numerical Control Co., Ltd. Wuhan, China) (Ref 37) was selected to get the thermal images of substrate and sprayed coating when damage occurred.

Figure 10 shows that the temperature field of substrate before spraying is nonuniform. There are local high- and low-temperature areas, corresponding to the high light and the gray color in the infrared thermal image, respectively. The major distribution is around 200 °C, and the difference is 70 °C between the maximum and the minimum among the substrate surface. Due to the nonuniform temperature distribution and the large quantity of heat input from the plasma jet with the short spray distance between the plasma gun and the substrate, the temperature difference cannot be avoided in spraying without an assisted cooling system; consequently, coating damage will occur.

Since the contribution of the sprayed particles is much more focused and gives rise to a large increase in the maximum transient temperature of the substrate surface (Ref 38), the local region in the sprayed coating would have a sharply increasing trend. When the coating damage occurs, the temperature curve will present an abnormal fluctuation due to the accumulation of large heat without efficient heat exchange between coating and substrate. This case can be used as a reference for diagnostic instrument and also as an initiation point for coating damage phenomenon.

The substrate was sprayed and coating damage happened after 180 s, and the thermal image taken when coating damage occurred is shown in Fig. 11. The conclusions can be drawn that the regions of coating damage

are in the higher-temperature area and the transition area from the higher temperature to the lower after comparing the same regions in Fig. 10 and Fig. 11. It can be seen from Fig. 12 that the variation of the average value has a steadily increasing trend from 140 to 192 °C during the spraying process. However, the mutation trend of the last cycle with coating damage for the standard deviation is 9 °C (the maximum is 39 °C), and the case for the average is 16 °C. The abnormal result agrees well with the supposition and the analysis above for the spraying process with coating damage.

3.3 Discussion

As for the time-integrated temperatures of substrate and sprayed coating, it is impossible to monitor their fluctuations using one fixed IR pyrometer without some kind of movements. Experimental results above demonstrate that the successive monitoring can be achieved with the help of the pyrometer and the robot scanning mechanism. Therefore, the measurement approach presented in the paper enlarges the detecting scope of the device and improves the system flexibility of the temperature-monitoring system. Furthermore, the robot spray trajectory illustrated in Fig. 3 can be adjusted during the spraying process, such as switching of new scanning step and starting point, to change the scanning track of IR pyrometer for more temperature information of the spraying targets.

In addition, experimental results also indicate that the two specific factors can be used to evaluate time-varied temperature and its fluctuation. There are steady average temperatures with a small ascending step and the slight fluctuation of standard deviations for the normal spraying process. However, it is not the case for the spraying process with coating damage. Coating damages always occur with high temperature gradient and resulting residual stress level (Ref 24, 39). Therefore, the standard deviation will exhibit an abnormal fluctuation as well as the average temperature.

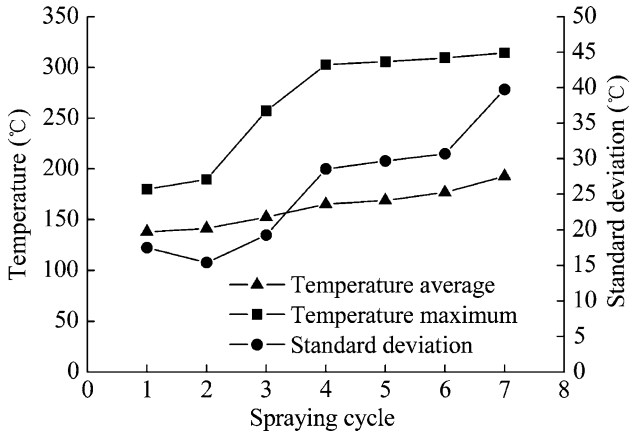

Fig. 12 Variations of the specific factors during the spraying process with coating damage

4. Influence of Robot Spray Trajectory Parameters on Coating Temperature

4.1 Spray Distance

Spray distance influences the coating quality (Ref 40) through the control of the particle flight duration and hence through their in-flight characteristics, in terms of temperature and velocity. In addition, heat transfers from plasma jet and spray particles to the substrate are sensitive to the spray distance. When the spray distance is short enough, the high-temperature scope of plasma jet can touch the substrate surface, thus resulting in the overheating of the target substrate (Ref 41).

As shown in Fig. 13, the temperature fluctuation becomes higher due to the higher heat input from plasma jet with respect to the smaller spray distance. However, when the spray distance is more than or equal to 200 mm, the temperature fluctuation becomes smaller because of the lower heat transfer and the efficient heat exchange between the mild steel plate substrate and sprayed coatings. Moreover, the fluctuation is gradually trending down with the increase of the spray distance.

As a whole, the heating effect of plasma jet and particle flux on substrates and previously sprayed coatings are varied with different spray distance. It is demonstrated in Fig. 14 that the periodic average temperature decreases with the increase of spray distance and vice versa. Variations in periodic average temperature show a function of spray distance, which agrees well with the result of rapid decrease of the maximum thermal flux transferred from plasma jet to substrate when the spray distance is increased (Ref 38, 42). There is a mostly constant temperature rise for each spray distance with respect to the other fixed spraying condition. This phenomenon may be explained by the steady net heat input to substrate and sprayed coating with the dynamic power balance of the spray condition.

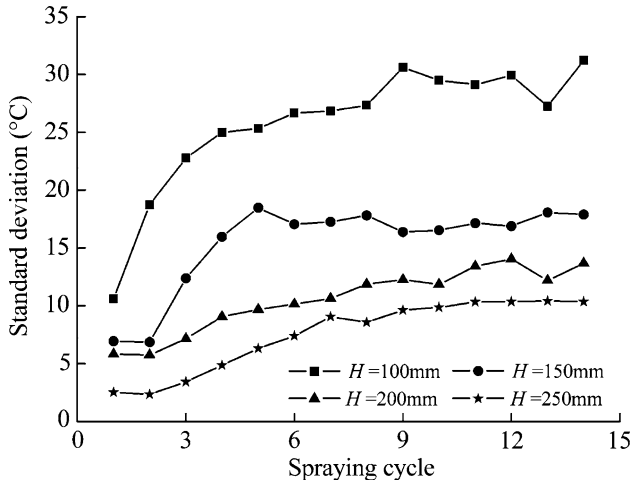

Fig. 13 Influence of spray distance on coating temperature fluctuation

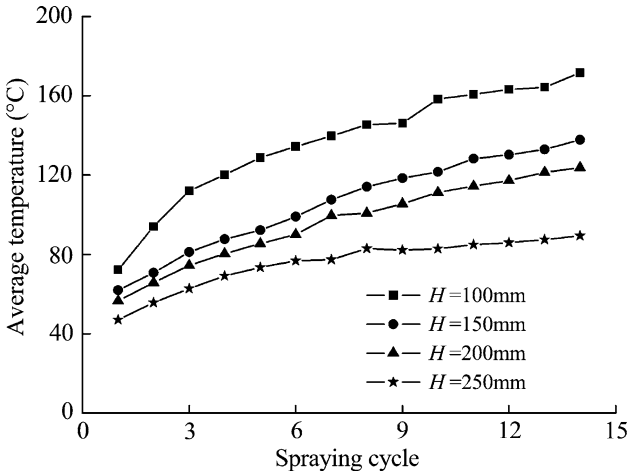

Fig. 14 Influence of spray distance on coating average temperature

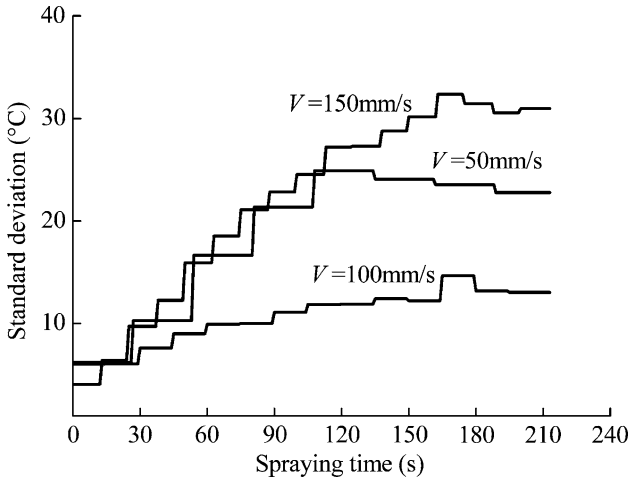

Fig. 15 Influence of scanning velocity on coating temperature fluctuation

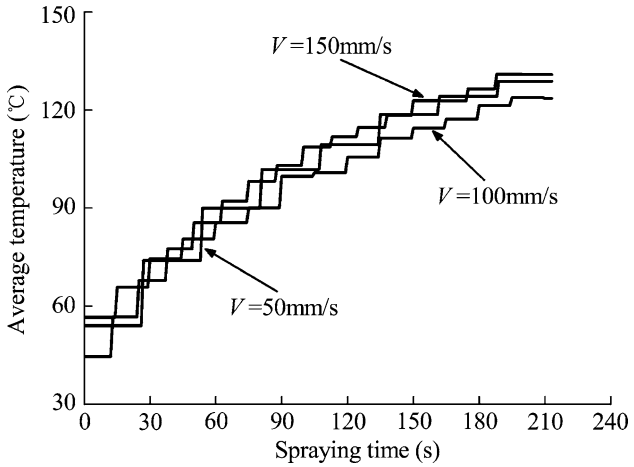

Fig. 16 Influence of scanning velocity on coating average temperature

The comparison of Fig. 13 and 14 shows that the operating situation with the spray distance of more than 200 mm is suitable for the preheating of metal substrates. This is because of two facets: relatively rapid increase of periodic average temperature but narrow temperature fluctuation, which can mitigate the development of thick oxide layer on the surface of metal or alloy samples sprayed in air.

4.2 Scanning Velocity

Scanning velocity and scanning step are the key parameters that particularly influence the deposit microstructure characteristics and the thermal exchanges since they control, for a given feedstock rate, the deposited thickness per pass (Ref 43). Different spray velocities of 50, 100, and 150 mm/s were selected for the experiments, and the corresponding spraying periods were 30, 17, and 11 s, respectively. It can be observed from Fig. 15 that temperature variations for different velocities apparently become differential after the spraying time of 60 s, and variations of 50 and 150 mm/s are higher than that of 100 mm/s. On the assumption that the net power output of the plasma power resource is constant and the influence of the spraying condition on heat transfer is the same, the heat transferred from the plasma gun to the substrate and sprayed coating is in direct proportion to the resident time of the plasma gun in the scope of substrate. Therefore, there are no significant differences between average temperatures for different spray velocities shown in Fig. 16, owing to the same heating time of plasma gun during the same spraying period. However, the temperature rise per spraying scan with the scanning velocity of 50 mm/s is higher than the others of 100 and 150 mm/s.

It is worth noting that the experimental results are partially different from the conclusions reported by Bao et al. (Ref 30). They considered that increasing the scanning velocity reduces the temperature fluctuations during a given spraying cycle, but does not change the overall temperature rise of the coating based on the comparison of the temperature variation of the two points calculated by the heat transfer model. However, it cannot be determined from their study that temperature fluctuations decrease with the increase of scanning velocity, but the overall temperature rise is almost constant. Their conclusions may be more reasonable, if they had taken the heat exchange between substrate and sprayed coating and the temperature distribution of the entire substrate sheet into consideration.

To summarize, the thickness of deposited coating per spraying cycle will become thicker with the lower scanning velocity. When the scanning velocity deceases, the large amounts of heat carried by particle flux is transferred to the substrate and coatings, which results in large temperature rise per spraying cycle. Meanwhile, the temperature gradients will increase, resulting in significantly high thermal stress and relaxation levels, which are not beneficial to the formation of coatings. Taking into account all of aforementioned considerations, there should exist a reasonable

choice of scanning velocity with respect to the steady average temperature and fluctuation. It is found that the scanning velocity of 100 mm/s is the optimized option for the given processing condition and the selected substrate.

4.3 Scanning Step

Different scanning steps of 5, 10, and 15 mm were selected for the experimental trials with respect to the corresponding spraying periods: 28, 15, and 13 s, respectively. As for the same spraying scope, robot spray trajectories were designed independently, and the focusing times of spray gun on the substrate during the unit time T were T_1, T_2, and T_3 respectively, in accord with the relationship of $T_2 < T_1 < T_3$.

It can be observed from Fig. 17 that temperature fluctuations decrease with the increase of the scanning step because the overlap of deposited particles is higher with smaller scanning step and the heat carried by the particles is accumulated within the sprayed zone. Therefore, the higher-temperature fluctuation is observed in the temperature curve for the scanning step of 5 mm. As shown in Fig. 18, the average temperature for the step of 10 mm is higher than those for other steps due to the longer heating time of spray jet and particle flux. There is no definitive relationship between the variation of average temperature and scanning step.

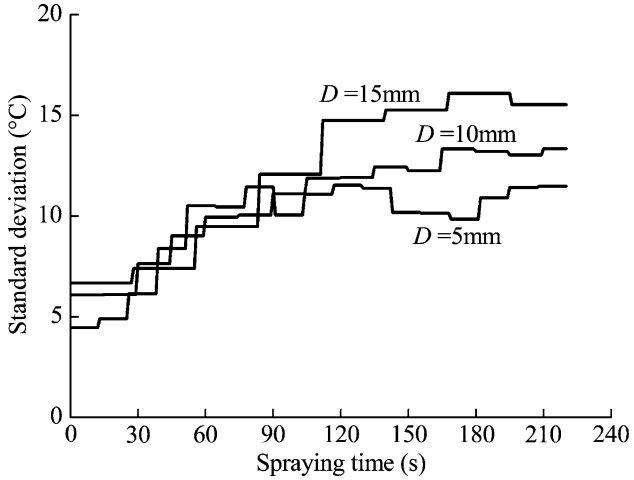

Fig. 17 Influence of scanning step on coating temperature fluctuation

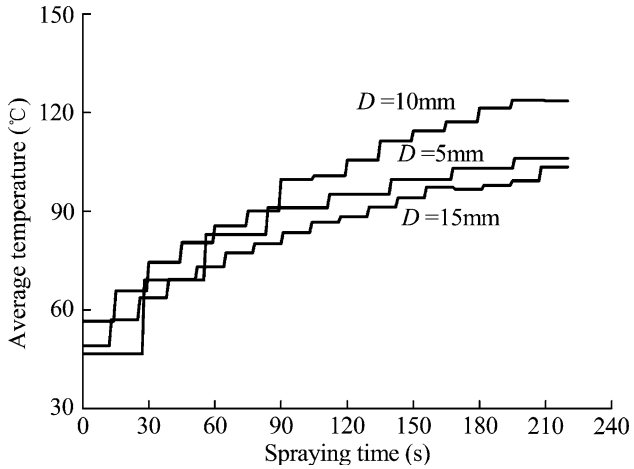

Fig. 18 Influence of scanning step on coating average temperature

5. Conclusions

In order to improve the process quality and reliability of plasma spray, an integrated temperature investigation approach for coating temperature measurement and control by IR pyrometer is presented in this paper. The present approach enlarges the detection scope of the device and improves the system flexibility of the temperature-monitoring system. Two specific factors, periodic average temperature and standard deviation, were adopted to evaluate the temperature variation and the fluctuation of the thermal cycle relevant to one robot scanning cycle based on the statistical method. These two factors were successful in describing the temperature history and variation during experimental processing sets, which is helpful for the real-time monitoring and control of coating temperature.

Experimental results show that average temperature has no evident difference as a function of scanning velocity and no fixed correlation with scanning step, but is dominated only by the heating time of plasma jet and particle flux. Therefore, the choice of optimal scanning velocity just needs to take account of temperature fluctuation. The temperature fluctuation decreases with the increasing of scanning step, but both average temperature and fluctuation decrease with the increasing of spray distance and vice versa.

This study also demonstrates that IR pyrometry combined with specific robot scanning trajectories allows temperature mapping of large sprayed targets. How to develop the integrated process control and diagnosis system of sprayed coating temperature combining IR pyrometer with thermal camera still needs further study.

Acknowledgment

Authors gratefully acknowledge the contribution of the "863" project from the Ministry of Science and Technology (2007AA04Z142), as well as that of the National Nature Science Foundation of China (Grant No. 50475134 and 50675081). In particular, thanks is given for the contribution of the Analytical and Testing Center of the Huazhong University of Science & Technology.

References

1. P. Fauchais, Understanding Plasma Spraying, *J. Phys. D: Appl. Phys.*, 2004, **37**(9), p R86-R108
2. P. Fauchais, A. Vardelle, and B. Dussoubs, Quo Vadis Thermal Spraying?, *J. Therm. Spray Technol.*, 2001, **10**(1), p 44-66

3. C. Moreau, Towards a Better Control of Thermal Spray Process, *Thermal Spray: Meeting the Challenges of the 21st Century*, C. Coddet, Ed., May 25-29, 1998 (Nice, France), ASM International, 1998, p 1681-1693
4. T. Renault, C. Bossoutrot, F. Braillard, S. Bansard, M. Vardelle, and P. Fauchais, A Reliable and Reproducible Plasma Spray Process using On-line Control, *Proceedings of Matériaux 2002*, 21-25 October, 2002 (Tours, France)
5. P. Fauchais and M. Vardelle, How to Improve the Reliability and Reproducibility of Plasma Sprayed Coatings, *Thermal Spray 2003: Advancing the Science and Applying the Technology*, B.R. Marple and C. Moreau, Eds., May 5-8, 2003 (Orlando, FL), ASM International, 2003, Vol. 2, p 1165-1173
6. T. Renault, M. Vardelle, P. Fauchais, H. Hoffmann, and F. Braillard, On-line Monitoring (SDC) through Coating Surface Temperature of Residual Stresses in APS WC-Co 17 wt% Coatings on Hastelloy X, *Thermal Spray 2001: New Surfaces for a New Millennium*, C.C. Berndt, K.A. Khor, and E.F. Lugscheider, Eds., May 28-30, 2001 (Singapore), ASM International, 2001, p 743-750
7. C. Verdy, B. Serio, and C. Coddet, In-situ Temperature Measurement using Embedded Micro-Thermocouples in Vacuum Plasma Sprayed Multi-Layered Structures, *Thermal Spray: Meeting the Challenges of the 21st Century*, C. Coddet, Ed., May 25-29, 1998 (Nice, France), ASM International, 1998, p 821-824
8. T. Grinys, S. Tamulevičius, and M. Žadvydas, Control of the Substrate Temperature during Plasma Spray Deposition, *Mater. Sci. (Medžiagotyra)*, 2004, **10**(3), p 221-224
9. H.W. Ng and Z. Gan, A Finite Element Analysis Technique for Predicting As-Sprayed Residual Stresses Generated by the Plasma Spray Coating Process, *Finite Elem. Anal. Des.*, 2005, **41**(13), p 1235-1254
10. P.H. Bertrand, M. Ignatiev, G. Flamant, and I. Smurov, Pyrometry Applications in Thermal Plasma Processing, *Vacuum*, 2000, **56**(1), p 71-76
11. P. Jokinen, T. Varis, A. Korpiola, and T. Kauppinen, In-situ Temperature Control of Coating and Workpiece in Thermal Spraying, *Tagungsband Conference Proceedings*, E. Lugscheider, and R.A. Kammer, Eds., March 17-19, 1999 (Düsseldorf, Germany), DVS Deutscher Verband für Schweißen, 1999, p 318-320
12. E. Lugscheider, F. Ladru, V. Gourlaouen, and C. Gualco, Enhanced Atmospheric Plasma Spraying of Thick TBCs by Improved Process Control and Deposition Efficiency, *Thermal Spray: Meeting the Challenges of the 21st Century*, C. Coddet, Ed., May 25-29, 1998 (Nice, France), ASM International, 1998, p 1583-1588
13. O. Brandt and M. Wandelt, Thermal Measurements of Substrate During Spray Processes, *Thermal Spray: Practical Solutions for Engineering Problems*, C.C. Berndt, Ed., Oct. 7-11, 1996 (Cincinnati, OH), ASM International, 1996, p 799-802
14. L. Moulla, Z. Salhi, M. P. Planche, M. Cherigui, C. Coddet, and F. Belfort, On the Measurement of Substrate Temperature during Thermal Spraying, *Thermal Spray Connects: Explore its Surfacing Potential*!, E. Lugscheider, Ed., May 2-4, 2005 (Basel, Switzerland), DVS-Verlag, Düsseldorf, Germany, 2005, p 679-683
15. J. P. Sauer and P. Sahoo, HVOF Process Control Using Almen and Temperature Measurement, *Thermal Spray 2001: New Surfaces for a New Millennium*, C.C. Berndt, K.A. Khor, and E.F. Lugscheider, Eds., May 28-30, 2001 (Singapore), ASM International, 2001, p 791-796
16. M. Dvorak, C. Florin, and E. Amrhein, On-line Quality Control of Thermally Sprayed Coatings, *Thermal Spray 2001: New Surfaces for a New Millennium*, C.C. Berndt, K.A. Khor, and E.F. Lugscheider, Eds., May 28-30, 2001 (Singapore), ASM International, 2001, p 1255-1259
17. P. Litoš, M. Honner, and J. Kuneš, Thermography Applications in Technology Research, *Proc. Infrared Camera Applications International Conference*, M.N. Billerica, Ed., Oct 4-8, 2004 (Las Vegas, NV), Infrared Training Center, 2004, p 321-330
18. D.R. Green, M.D. Schmeller, and R.A. Sulit, Thermal Nondestructive Examination Method for Thermal Sprayed Coatings, *Oceans*, 1982, **14**, p 532-536
19. P. Jokinen, T. Kauppinen, T. Varis, and K. Korpiola, Using IR-Thermography as a Quality-Control Tool for Thermal Spraying in the Aircraft Industry, *Proc. SPIE— The International Society for Optical Engineering*, R.B. Dinwiddie and D.H. Lemieux, Eds., April 24-27, 2000 (Orlando, FL), Society of Photo-Optical Instrumentation Engineers, 2000, p 232-237
20. P.D.A. Jones, S.R. Duncan, T. Rayment, and P.S. Grant, Control of Temperature Profile for a Spray Deposition Process, *IEEE Transactions on Control Systems Technology*, 2003, **11**(5), p 656-667
21. E. Lugscheider, F. Ladru, A. Fischer, and C. Herbst, Plasma Sprayed Ceramic Coatings for Electrical Purposes - Necessity of Process Control, *Proc. 24th Annual Conference of the IEEE Industrial Electronics Society*, Aug 31-Sept 4, 1998 (Aachen, Germany), Institute of Electrical & Electronics Enginee 1998, p 2284-2289
22. Y. Cheng, *In situ Practicality Technology of Infrared Diagnosis.* Mechanical Industry Publish House, Beijing, China, 2002, p 3-4, (in Chinese)
23. C.J. Friedrich, R. Gadow, A. Killinger, and C. Li, IR Thermographic Imaging—A Powerful Tool for On-line Process Control of Thermal Spraying, *Thermal Spray 2001: New Surfaces for a New Millennium*, C.C. Berndt, K.A. Khor, and E.F. Lugscheider, Eds., May 28-30, 2001 (Singapore), ASM International, 2001, p 779-786
24. H. Zhang, H. Liu, G. Wang, and M. Guo, Experimental Research on Temperature Field of Plasma Spray Coating, *China Mechanical Engineering*, 2004, **15**(21), p 1958-1961, (in Chinese)
25. K. Richter and K. Drescher, Pyrometric Substrate Temperature Measurement during Plasma Etching, *Surf. Coat. Technol.*, 1995, **74-75**(1-3), p 546-551
26. T. Renault, M. Vardelle, A. Grimaud, P. Fauchais, and H. Hoffman, On-line Control of Particle Spray Jet and Residual Stresses in Plasma Sprays, *Thermal Spray: Surface Engineering via Applied Research*, C.C. Berndt, Ed., May 8-11, 2000 (Montréal, Québec, Canada), ASM International, 2000, p 1383-1391
27. C. Bossoutrot, F. Braillard, S. Bansard, M. Vardelle, and P. Fauchais, Industrial On-line Control of HVOF Spray Process using SDC System, *Thermal Spray 2003: Advancing the Science and Applying the Technology*, B.R. Marple, and C. Moreau, Eds., May 5-8, 2003 (Orlando, FL), ASM International, 2003, Vol. 2, p 1165-1173
28. E. Meillot and E.M. Fromentin, Measurements of Heat Flux in an Atmosphere- and Temperature-Controlled Plasma Spray Process, *Ann. N.Y. Acad. Sci.*, 1999, **891**(1), p 90-97
29. E. Meillot, L. Bianchi, E. Roussel, and A. Freslon, Industrial Applications with the Atmosphere and Temperature Controlled Plasma Spraying Process, *High Temp. Mater. Proc.*, 2001, **5**(1), p 51-59
30. Y. Bao, T. Zhang, and D.T. Gawne, Non-Steady State Heating of Substrate and Coating During Thermal Spray Deposition, *Surf. Coat. Technol.*, 2005, **194**(1), p 82-90
31. M. Vardelle, T. Renault, and P. Fauchais, Choice of an IR Pyrometer to Measure the Surface Temperature of a Coating during its Formation in Air Plasma Spraying, *High Temp. Mater. Proc.*, 2002, **6**(4), p 469-489
32. "Raytek Automation Products: Noncontact Temperature Measurement for Industrial Applications," 2-2102 Rev. D, Raytek Corporation, March 2006
33. H. Madura and T. Piatkowski, Emissivity Compensation Algorithms in Double-Band Pyrometry, *Infrared Phys. Technol.*, 2004, **46**(1-2), p 185-189
34. L. Moulla, P. Gougeon, and C. Coddet, Influence of Reflected Atmospheric Plasma Spraying Torch Radiations on Long Wavelength Ir Radiometry Temperature Measurement, *Infrared Phys. Technol.*, 2005, **46**(5), p 364-369
35. L. Chen, T. Bing, and X. Hu, Design Principle for Simultaneous Emissivity and Temperature Measurements, *Opt. Eng.*, 1990, **29**(12), p 1445-1448
36. M. Schlessinger, *Infrared Technology Fundamentals*, Marcel Dekker, 1995, p 12
37. "Technical Parameters of HY-2188G IR Thermal Camera," Infrared Department of Huazhong Numerical Control Co., Ltd., Wuhan, China, Undated

38. R. Bolot, L. Li, R. Bonnet, C. Mateus, and C. Coddet, Modeling of the Substrate Temperature Evolution during the APS Thermal Spray Process, *Thermal Spray 2003: Advancing the Science and Applying the Technology*, B.R. Marple, and C. Moreau, Eds., May 5-8, 2003 (Orlando, FL), ASM International 2003, Vol. 2, p 949-954
39. L. Bianchi, N. Baradel, I.N. Liorca, and V.G. Bertran, Influence of Plasma Spraying Parameters on Coating Damage, *Thermal Spray: Surface Engineering via Applied Research*, C.C. Berndt, Ed., May 8-11, 2000 (Montréal, Québec, Canada), ASM International, 2000, p 29-36
40. S.L. Chen, P. Sitonen, and P. Kettunen, Experimental Design and Parameter Optimization for Plasma Spraying of Alumina Coatings, *Thermal Spray: International Advances in Coatings Technology*, C.C. Berndt, Ed., 1992 (Orlando, FL), ASM International, 1992, p 51-56
41. B. Xu, S. Liu, and X. Liu, Plasma Spray and Bead Weld. China Railway Press, Beijing, 1986, p 61-62, (in Chinese)
42. R. Bolot, M. Imbert, and C. Coddet, Three Dimensional Transient Modeling of the Substrate Temperature Evaluation during the Coating Elaboration, *Tagungsband Conference Proc.*, E. Lugscheider, Ed., March 4-6, 2002 (Essen, Germany), DVS Deutscher Verband Fur SchweiBen, 2002, p 979-984
43. S. Guessasma, G. Montavon, and C. Coddet, Modeling of the APS Plasma Spray Process using Artificial Neural Networks: Basis, Requirements and an Example, *Comput. Mater. Sci.*, 2004, **29**(3), p 315-333